wjert, 2024, Vol. 10, Issue 5, 127-147. Original Article ISSN 2454-695X

World Journal of Engineering Research and Technology
WJERT
www.wjert.org
SJIF Impact Factor: 7.029

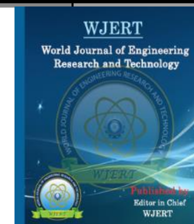

MAXIMAL EFFICIENCIES IN -ALLOY JUNCTION SOLAR CELLS AT 300 K, ACCORDING TO HIGHEST HOT RESERVOIR TEMPERATURES, OBTAINED FROM CARNOT-EFICIENCY THEOREM. (VI)

Prof. Dr. Huynh Van Cong*

Université de Perpignan Via Domitia, Laboratoire de Mathématiques et Physique (LAMPS), EA 4217, Département de Physique, 52, Avenue Paul Alduy, F-66 860 Perpignan, France.

Article Received on 01/04/2024 **Article Revised on 21/04/2024** **Article Accepted on 11/05/2024**

***Corresponding Author**
Prof. Dr. Huynh Van Cong
Université de Perpignan Via Domitia, Laboratoire de Mathématiques et Physique (LAMPS), EA 4217, Département de Physique, 52, Avenue Paul Alduy, F-66 860 Perpignan, France.

ABTRACT

In $n^{+}(p^{+}) - p(n)$ $[X(x) \equiv GaP_{1-x}As_{x}]$-alloy junction solar cells at T=300 K, $0 \leq x \leq 1$, by basing on the same physical model and the same treatment method, as those used in our recent works[1,2], we will also investigate the maximal efficiencies, $\eta_{Imax.(IImax.)}$, obtained at the open circuit voltage $V_{oc}(= V_{ocI(ocII)})$, according to highest hot reservoir temperatures, $T_H(K)$, obtained from the Carnot efficiency theorem, which was demonstrated by the use of the entropy law. In this word, some concluding remarks are given in the following. **(1)** In the heavily doped emitter region, the effective density of electrons (holes), N^{*}, given in parabolic conduction (valence) bands, expressed as functions of the total dense impurity density, N, donor (acceptor)-radius, $r_{d(a)}$, and x-concentration, is defined in Eq. (9d), as: $N^{*}(N, r_{d(a)}, x) \equiv N - N_{CDn(NDp)}(r_{d(a)}, x)$, where $N_{CDn(NDp)}$ is the Mott critical density in the metal-insulator transition, determined in Eq. (9a). Then, we have showed that (i) the origin of such the Mott's criterium, Eq. (9a), is exactly obtained from the reduced effective Wigner-Seitz radius $r_{sn(sp)}$, characteristic of interactions, as that given in Equations (9b, 9c), and further (ii) $N_{CDn(CDp)}$ is just the density of electrons (holes) localized in the exponential conduction (valence)-band tail (EBT), as that demonstrated in[1] **(2)** In Table 3n, for

$n^+ - p\ X(x)$ −alloy junction solar cell and for $r_{Sn(Cd)}$-radius, one obtains with increasing x=(0, 0.5, 1): $\eta_{Imax.}(\searrow)$= **32.83%**, 31.96%, 31.15%, according to $T_H(\searrow) = \mathbf{446.6\ K}, 440.9\ K, 435.7\ K$, at $V_{ocI} = \mathbf{1.06\ V}, 1.06\ V, 1.07\ V$, respectively. **(3)** In Table 5p, for $p^+ - n\ X(x)$ −alloy junction solar cell and for $r_{Cd(Sn)}$-radius, with increasing x=(0, 0.5, 1), one obtains with increasing x=(0, 0.5, 1): $\eta_{IImax.}(\nearrow)$= 32.51%, 32.51%, **33.07%**, according to $T_H(\nearrow) = 444.5\ K, 444.5\ K, \mathbf{448.2\ K}$, at $V_{ocII}(V)[> V_{ocI}(V)] = 1.17\ V, 1.18\ V, 1.20\ V$, respectively, suggesting that such $\eta_{Imax.(IImax.)}$-and-T_H variations depend on $V_{ocII}(V)[> V_{ocI}(V)] -$ ones. **(4)** Finally, as discussed in above remarks (2) and (3), for x=1, the $GaP_{1-x}As_x$ −alloy becomes the GaAs-one, and therefore, $\eta_{Imax.}$=31.15 % and $\eta_{IImax.}$=33.07 %, which can be compared with the corresponding results obtained by Moon et al.[6] and Green et al.[4] for the single-junction GaAs thin-film solar cell, 22.08 % and 29.71 %, respectively, suggesting that in order to obtain the highest efficiencies, the $GaP_{1-x}As_x$-alloy junction solar cells could be chosen rather than the crystalline GaAs-junction solar cell.

KEYWORDS: single $GaP_{1-x}As_x$-alloy junction solar cell; single crystalline GaAs-junction solar cell; photovoltaic conversion factor; photovoltaic conversion efficiency.

INTRODUCTION

In single $n^+(p^+) - p(n)\ X(\equiv GaP_{1-x}As_x)$-alloy junction solar cells at 300 K, $0 \le x \le 1$, by basing on the same physical model and treatment method, as used in our two recent works[1,2], and also on other ones [2-11], we will investigate the highest (or maximal) efficiencies, $\eta_{Imax.(IImax.)}$, according to highest hot reservoir temperatures $T_H(K)$, obtained from the Carnot- efficiency theorem, being proved by the entropy law.

In the following, we will show that the energy-band-structure parameters, due to the effects of x-concentration, size impurity, temperature T and heavy doping, affect strongly the dark (or total) minority-carrier saturation current density and the photovoltaic conversion effect.

ENERGY BAND STUCTURE PARAMETERS

A. Effect of x- concentration

In the $n^+(p^+) - p(n)$ single $n^+(p^+) - p(n)\ X(x)$- alloy junction at T=0 K, the energy-band-structure parameters[1], are expressed as functions of x, are given in the following.

(i)-The unperturbed relative effective electron (hole) mass in conduction (valence) bands are given by:

$m_c(x)/m_o = 0.066 \times x + 0.13 \times (1-x)$, and

$m_v(x)/m_o = 0.291 \times x + 0.5 \times (1-x)$, (1)

so that one obtains: $m_c(x=1)/m_o = (m_{c(GaAs)}/m_o)$=0.066, $m_v(x=1)/m_o = (m_{v(GaAs)}/m_o)$=0.291, and $m_c(x=0)/m_o = (m_{c(GaP)}/m_o)$=0.13, $m_v(x=0)/m_o = (m_{v(GaP)}/m_o)$=0.5.

(ii)-The unperturbed relative static dielectric constant of the intrinsic of the single crystalline X- alloy is found to be defined by:

$\varepsilon_o(x) = 13.13 \times x + 11.1 \times (1-x)$, (2)

which gives: $\varepsilon_o(x=1) = \varepsilon_{GaAs}$=13.13, and $\varepsilon_o(x=0) = \varepsilon_{GaP} = 11.1$.

(iii)-Finally, the unperturbed band gap at 0 K is found to be given by:

$E_{go}(x)$ in eV $= 1.52 \times x + 1.796 \times (1-x)$, (3)

giving rise to: $E_{gio}(x=1) = E_{gGaAs} = 1.52$ eV, and $E_{gio}(x=0) = E_{gGaP} = 1.796$ eV.

Therefore, we can define the effective donor (acceptor)-ionization energy, at $r_{d(a)} = r_{do(ao)} = r_{P(Ga)} = 0.11$ nm (0.126 nm), in absolute values as:

$$E_{do(ao)}(x) = \frac{13600 \times [m_{c(v)}(x)/m_o]}{[\varepsilon_o(x)]^2} \text{ meV}, \quad (4)$$

and then, the isothermal bulk modulus, by:

$$B_{do(ao)}(x) \equiv \frac{E_{do(ao)}(x)}{\left(\frac{4\pi}{3}\right) \times \left(r_{do(ao)}\right)^3}. \quad (5)$$

B. Effects of Impurity-size, with a given x

Here, the effects of $r_{d(a)}$ and x- concentration affect the changes in all the energy-band-structure parameters, expressed in terms of the effective relative dielectric constant $\varepsilon(r_{d(a)}, x)$, in the following.

At $r_{d(a)} = r_{do(ao)}$, the needed boundary conditions are found to be, for the impurity-atom volume V= $(4\pi/3) \times \left(r_{d(a)}\right)^3$, $V_{do(ao)} = (4\pi/3) \times \left(r_{do(ao)}\right)^3$, for the pressure p, $p_o = 0$, and for the deformation potential energy (or the strain energy) σ, $\sigma_o = 0$. Further, the two important equations (Van Cong et al., 1984), used to determine the σ-variation, Δσ≡

$\sigma - \sigma_o = \sigma$, are defined by: $\frac{dp}{dV} = -\frac{B}{V}$ and $p = -\frac{d\sigma}{dV}$. giving: $\frac{d}{dV}(\frac{d\sigma}{dV}) = \frac{B}{V}$. Then, by an integration, one gets:

$$[\Delta\sigma(r_{d(a)}, x)]_{n(p)} = B_{do(ao)}(x) \times (V - V_{do(ao)}) \times \ln\left(\frac{V}{V_{do(ao)}}\right) = E_{do(ao)}(x) \times \left[\left(\frac{r_{d(a)}}{r_{do(ao)}}\right)^3 - 1\right] \times \ln\left(\frac{r_{d(a)}}{r_{do(ao)}}\right)^3 \geq 0. (6)$$

Furthermore, we also shown that, as $r_{d(a)} > r_{do(ao)}$ ($r_{d(a)} < r_{do(ao)}$), the compression (dilatation) gives rise to the increase (the decrease) in the energy gap $E_{gn(gp)}(r_{d(a)}, x)$, and the effective donor (acceptor)-ionization energy $E_{d(a)}(r_{d(a)}, x)$ in absolute values, obtained in the effective Bohr model, which is represented respectively by: $\pm [\Delta\sigma(r_{d(a)}, x)]_{n(p)}$,

$$E_{gn(gp)}(r_{d(a)}, x) - E_{go}(x) = E_{d(a)}(r_{d(a)}, x) - E_{do(ao)}(x) = E_{do(ao)}(x) \times \left[\left(\frac{\varepsilon_o(x)}{\varepsilon(r_{d(a)})}\right)^2 - 1\right] = + [\Delta\sigma(r_{d(a)}, x)]_{n(p)},$$

for $r_{d(a)} \geq r_{do(ao)}$, and for $r_{d(a)} \leq r_{do(ao)}$,

$$E_{gn(gp)}(r_{d(a)}, x) - E_{go}(x) = E_{d(a)}(r_{d(a)}, x) - E_{do(ao)}(x) = E_{do(ao)}(x) \times \left[\left(\frac{\varepsilon_o(x)}{\varepsilon(r_{d(a)})}\right)^2 - 1\right] = - [\Delta\sigma(r_{d(a)}, x)]_{n(p)}. (7)$$

Therefore, from Equations (6) and (7), one obtains the expressions for relative dielectric constant $\varepsilon(r_{d(a)}, x)$ and energy band gap $E_{gn(gp)}(r_{d(a)}, x)$, as:

(i)-for $r_{d(a)} \geq r_{do(ao)}$, since $\varepsilon(r_{d(a)}, x) = \frac{\varepsilon_o(x)}{\sqrt{1 + \left[\left(\frac{r_{d(a)}}{r_{do(ao)}}\right)^3 - 1\right] \times \ln\left(\frac{r_{d(a)}}{r_{do(ao)}}\right)^3}} \leq \varepsilon_o(x)$,

$$E_{gn(gp)}(r_{d(a)}, x) - E_{go}(x) = E_{d(a)}(r_{d(a)}, x) - E_{do(ao)}(x) = E_{do(ao)}(x) \times \left[\left(\frac{r_{d(a)}}{r_{do(ao)}}\right)^3 - 1\right] \times \ln\left(\frac{r_{d(a)}}{r_{do(ao)}}\right)^3 \geq 0, (8a)$$

according to the increase in both $E_{gn(gp)}(r_{d(a)}, x)$ and $E_{d(a)}(r_{d(a)}, x)$, for a given x, and

(ii)-for $r_{d(a)} \leq r_{do(ao)}$, since $\varepsilon(r_{d(a)}, x) = \frac{\varepsilon_o(x)}{\sqrt{1 - \left[\left(\frac{r_{d(a)}}{r_{do(ao)}}\right)^3 - 1\right] \times \ln\left(\frac{r_{d(a)}}{r_{do(ao)}}\right)^3}} \geq \varepsilon_o(x)$, with a condition, given by: $\left[\left(\frac{r_{d(a)}}{r_{do(ao)}}\right)^3 - 1\right] \times \ln\left(\frac{r_{d(a)}}{r_{do(ao)}}\right)^3 < 1$,

$$E_{gn(gp)}(r_{d(a)}, x) - E_{go}(x) = E_{d(a)}(r_{d(a)}, x) - E_{do(ao)}(x) = -E_{do(ao)}(x) \times \left[\left(\frac{r_{d(a)}}{r_{do(ao)}}\right)^3 - 1\right] \times \ln\left(\frac{r_{d(a)}}{r_{do(ao)}}\right)^3 \leq 0, (8b)$$

corresponding to the decrease in both $E_{gn(gp)}(r_{d(a)}, x)$ and $E_{d(a)}(r_{d(a)}, x)$, for a given x.

Furthermore, it is interesting to remark that the critical total donor (acceptor)-density in the metal-insulator transition (**MIT**) at T=0 K, $N_{CDn(NDp)}(r_{d(a)}, x)$, was given by the Mott's criterium, as:

$$N_{CDn(CDp)}(r_{d(a)}, x)^{1/3} \times a_{Bn(Bp)}(r_{d(a)}, x) = M_{n(p)},\ M_{n(p)} = 0.25, \quad (9a)$$

which can be explained from the definition of the reduced effective Wigner-Seitz (**WS**) radius $r_{sn(sp)}$, characteristic of interactions, by:

$$r_{sn(sp)}(N, r_{d(a)}, x) \equiv \left(\frac{3}{4\pi N}\right)^{1/3} \times \frac{1}{a_{Bn(Bp)}(r_{d(a)}, x)} = 1.1723 \times 10^{8} \times \left(\frac{1}{N}\right)^{1/3} \times \frac{m_{c(v)}(x)/m_o}{\varepsilon(r_{d(a)}, x)}, \quad (9b)$$

being equal to, in particular, at $N=N_{CDn(CDp)}(r_{d(a)}, x)$: $r_{sn(sp)}(N_{CDn(CDp)}(r_{d(a)}, x), r_{d(a)}, x)=$ **2.4814**, for any $(r_{d(a)}, x)$-values. So, from Eq. (9b), one has:

$$N_{CDn(CDp)}(r_{d(a)}, x)^{1/3} \times a_{Bn(Bp)}(r_{d(a)}, x) = \left(\frac{3}{4\pi}\right)^{1/3} \times \frac{1}{2.4814} = \mathbf{0.25} = (\mathbf{WS})_{n(p)} = \mathbf{M}_{n(p)}\,. \quad (9c)$$

In our recent paper[1], we have also showed that $N_{CDn(CDp)}$ is just the density of electrons (holes) localized in the exponential conduction (valence)-band tail (EBT), with a precision of the order of 2.92×10^{-7} . So, the density of electrons (holes) given in parabolic conduction (valence) bands can be defined by:

$$N^{*}(N, r_{d(a)}, x) \equiv N - N_{CDn(NDp)}(r_{d(a)}, x), \quad (9d)$$

which will be used in the n(p)-type degenerate X(x)-alloy, as follows.

C. Effect of temperature T, with given x and $r_{d(a)}$

Here, the intrinsic band gap $E_{gin(gip)}(r_{d(a)}, x, T)$ at any T is given by:

$$E_{gin(gip)}(r_{d(a)}, x, T) \text{ in eV} = E_{gn(gp)}(r_{d(a)}, x) - 10^{-4} \times T^{2} \times \left[\frac{5.405 \times x}{T+204} + \frac{3.065 \times (1-x)}{T+94}\right], \quad (10)$$

Which gives: $E_{gin(gip)}(r_{do(ao)}, x=0, T=0K) = 1.796$ eV and $E_{gin(gip)}(r_{do(ao)}, x=1, T=0K) = 1.52$ eV, and $E_{gin(gip)}(r_{do(ao)}, x=0, T=300\text{ K}) = 1.72599$ eV and $E_{gin(gip)}(r_{do(ao)}, x=1, T=300\text{ K}) = 1.42348$ eV, suggesting that, for given x and $r_{d(a)}$, $E_{gin(gip)}$ decreases with an increasing T, as observed in next Table 1 in Appendix 1.

Furthermore, in the n(p)-type X(x)-alloy, one can define the intrinsic carrier concentration $n_{in(ip)}$ by:

$$n^{2}_{i\,n(ip)}(r_{d(a)}, x, T) \equiv N_{c}(T, x) \times N_{v}(T, x) \times \exp\left(\frac{-E_{gin(gip)}(r_{d(a)}, x, T)}{k_{B}T}\right), \quad (11)$$

where $N_{c(v)}(T, x)$ is the conduction (valence)-band density of states, being defined as:

$$N_{c(v)}(T, x) = 2 \times \left(\frac{m_{c(v)}(x) \times k_{B}T}{2\pi\hbar^{2}}\right)^{\frac{3}{2}} (\text{cm}^{-3}).$$

D. Heavy Doping Effect, with given T, x and $r_{d(a)}$

Here, as given in our previous works[1,2], the Fermi energy $E_{Fn}(-E_{Fp})$, band gap narrowing (BGN), and apparent band gap narrowing (ABGN), are reported in the following.

First, the reduced Fermi energy $\eta_{n(p)}$ or the Fermi energy $E_{Fn}(-E_{Fp})$, obtained for any T and any effective d(a)-density, $N^*(N, r_{d(a)}, x) = N^*$, defined in Eq. (9d), for a simplicity of presentation, being investigated in our previous paper[8], with a precision of the order of 2.11×10^{-4}, is found to be given by:

$$\eta_{n(p)}(u) \equiv \frac{E_{Fn}(u)}{k_B T}\left(\frac{-E_{Fp}(u)}{k_B T}\right) = \frac{G(u)+Au^B F(u)}{1+Au^B},\ A = 0.0005372 \text{ and } B = 4.82842262, \quad (12)$$

where u is the reduced electron density, $u(N^*, T, x) \equiv \frac{N^*}{N_{c(v)}(T,x)}$, $F(u) = au^{\frac{2}{3}}\left(1 + bu^{-\frac{4}{3}} + cu^{-\frac{8}{3}}\right)^{-\frac{2}{3}}$,

$a = \left[(3\sqrt{\pi}/4) \times u\right]^{2/3}$, $b = \frac{1}{8}\left(\frac{\pi}{a}\right)^2$, $c = \frac{62.3739855}{1920}\left(\frac{\pi}{a}\right)^4$, and $G(u) \simeq Ln(u) + 2^{-\frac{3}{2}} \times u \times e^{-du}$;

$d = 2^{3/2}\left[\frac{1}{\sqrt{27}} - \frac{3}{16}\right] > 0.$

Here, one notes that: (i) as $u \gg 1$, according to the HD [d(a)- X(x)- alloy] ER-case, or to the degenerate case, Eq. (12) is reduced to the function F(u), and (ii) $\frac{E_{Fn}(u\ll1)}{k_B T}\left(\frac{-E_{Fp}(u\ll1)}{k_B T}\right) \ll -1$, to the LD [a(d)- X(x)- alloy] BR-case, or to the non-degenerate case, Eq. (12) is reduced to the function G(u). Here, the notations: HD(LD) and ER(BR), mean: heavily doped (lightly doped)-cases and emitter (base)-regions, respectively.

So, the numerical results of $B_{do(ao)}$, ε, $E_{gno(gpo)}$, $N_{CDn(CDp)}$, $E_{gin(gip)}(r_{d(a)}, x, T)$, and $\eta_{n(p)}(u)$, calculated using Equations (5), (8a, 8b), (9a), (10), and (12), respectively.

Table 1 in Appendix 1

Now, if denoting now the effective Wigner-Seitz radius $r_{sn(sp)}$, characteristic of the interactions, by:

$$r_{sn(sp)}(N^*, r_{d(a)}, x) = 1.1723 \times 10^8 \times \left(\frac{1}{N^*}\right)^{1/3} \times \frac{m_{c(v)}(x)}{\varepsilon(r_{d(a)}, x)}, \quad (13)$$

the correlation energy of an effective electron gas, $E_{cn(cp)}(N^*, r_{d(a)}, x)$, is given as[4]:

$$E_{cn(cp)}(N^*, r_{d(a)}, x) = \frac{-0.87553}{0.0908 + r_{sn(sp)}} + \frac{\frac{0.87553}{0.0908+r_{sn(sp)}} + \left(\frac{2[1-\ln(2)]}{\pi^2}\right) \times \ln(r_{sn(sp)}) - 0.093288}{1 + 0.03847728 \times r_{sn(sp)}^{1.67378876}}.$$

Now, taking into account various spin-polarized chemical potential-energy contributions such as (Van Cong, 2024): exchange energy of an effective electron (hole) gas, majority-carrier correlation energy of an effective electron (hole) gas, minority hole (electron) correlation energy, majority electron (hole)-ionized d(a) interaction screened Coulomb potential energy,

and finally minority hole (electron)-ionized d(a) interaction screened Coulomb potential energy, the band gap narrowing (BGN) are given as follows.

Thus, in the n-type HD X(x)- alloy, the BGN is found to be given by[2]:

$$\Delta E_{gn}(N^*, r_d, x) \simeq a_1 \times \frac{\varepsilon_0(x)}{\varepsilon(r_d,x)} \times N_r^{1/3} + a_2 \times \frac{\varepsilon_0(x)}{\varepsilon(r_d,x)} \times N_r^{\frac{1}{3}} \times (2.503 \times [-E_{cn}(r_{sn}) \times r_{sn}]) + a_3 \times \left[\frac{\varepsilon_0(x)}{\varepsilon(r_d,x)}\right]^{5/4} \times \sqrt{\frac{m_v}{m_c}} \times N_r^{1/4} + a_4 \times \sqrt{\frac{\varepsilon_0(x)}{\varepsilon(r_d,x)}} \times N_r^{1/2} \times 2 + a_5 \times \left[\frac{\varepsilon_0(x)}{\varepsilon(r_d,x)}\right]^{\frac{3}{2}} \times N_r^{\frac{1}{6}},$$

$$N_r \equiv \left(\frac{N^*}{N_{CDn}(r_d,x)}\right), \quad (14n)$$

Where $a_1 = 3.8 \times 10^{-3}(eV)$, $a_2 = 6.5 \times 10^{-4}(eV)$, $a_3 = 2.8 \times 10^{-3}(eV)$,$a_4 = 5.597 \times 10^{-3}(eV)$ and $a_5 = 8.1 \times 10^{-4}(eV)$, and in the p-type HD X(x)- alloy, as:

$$\Delta E_{gp}(N^*, r_a, x) \simeq a_1 \times \frac{\varepsilon_0(x)}{\varepsilon(r_a,x)} \times N_r^{1/3} + a_2 \times \frac{\varepsilon_0(x)}{\varepsilon(r_a,x)} \times N_r^{\frac{1}{3}} \times (2.503 \times [-E_{cp}(r_{sp}) \times r_{sp}]) + a_3 \times \left[\frac{\varepsilon_0(x)}{\varepsilon(r_a,x)}\right]^{5/4} \times \sqrt{\frac{m_c}{m_v}} \times N_r^{1/4} + 2a_4 \times \sqrt{\frac{\varepsilon_0(x)}{\varepsilon(r_a,x)}} \times N_r^{1/2} + a_5 \times \left[\frac{\varepsilon_0(x)}{\varepsilon(r_a,x)}\right]^{\frac{3}{2}} \times N_r^{\frac{1}{6}},$$

$$N_r \equiv \left(\frac{N^*}{N_{CDp}(r_a,x)}\right), \quad (14p)$$

Where $a_1 = 3.15 \times 10^{-3}(eV)$, $a_2 = 5.41 \times 10^{-4}(eV)$, $a_3 = 2.32 \times 10^{-3}(eV)$, $a_4 = 4.195 \times 10^{-3}(eV)$ and $a_5 = 9.80 \times 10^{-5}(eV)$.

Therefore, in the HD[d(a)- X(x)- alloy] ER, we can define the effective extrinsic carrier concentration, $n^*_{en(ep)}$, by :

$$n^*_{en(ep)}(N^*, T, r_{d(a)}, x) \equiv \sqrt{N^* \times p_o(n_o)} = n_{in(ip)}(T, r_{d(a)}, x) \times \exp\left[\frac{\Delta E_{agn(agp)}}{2k_B T}\right], \quad (15)$$

where the apparent band gap narrowing (ABGN), $\Delta E_{agn(agp)}$, is defined by:

$$\Delta E_{agn}(N^*, T, r_d, x) \equiv \Delta E_{gn}(N^*, r_d, x) + k_B T \times \ln\left(\frac{N^*}{N_c(T,x)}\right) - E_{Fn}(N^*, T, x), \quad (16n)$$

$$\Delta E_{agp}(N^*, T, r_a, x) \equiv \Delta E_{gp}(N^*, r_a, x) + k_B T \times \ln\left(\frac{N^*}{N_v(T,x)}\right) + E_{Fp}(N^*, T, x)]. \quad (16p)$$

TOTAL MINORITY-CARRIER SATURATION CURRENT DENSITY

In the two $n^+(p^+) - p(n)$ X(x)- alloy -junction solar cells, denoted respectively by I(II), the total carrier-minority saturation current density is defined by:

$$J_{oI(oII)} \equiv J_{Eno(Epo)} + J_{Bpo(Bno)} \quad (17)$$

where $J_{Bpo(Bno)}$ is the minority-electron (hole) saturation current density injected into the LD[a(d)- X(x)- alloy] BR, and $J_{Eno(Epo)}$ is the minority-hole (electron) saturation-current density injected into the HD[d(a)- X(x)- alloy] ER.

$J_{Bpo(Bno)}$ in the LD[a(d)- X(x)- alloy]BR

Here, $J_{Bpo(Bno)}$ is determined by[2]:

$$J_{Bpo(Bno)}\left(N_{a(d)},T,r_{a(d)},x\right)=\frac{e\times n_{ip(in)}^{2}(T,r_{a(d)},x)\times\sqrt{\frac{D_{e(h)}(N_{a(d)},T,r_{a(d)},x)}{\tau_{eB(hB)}(N_{a(d)})}}}{N_{a(d)}},\qquad(18)$$

where $n_{ip(in)}^{2}(T,r_{d(a)},x)$ is determined Eq. (11), $D_{e(h)}(N_{a(d)},T,r_{a(d)},x)$ is the minority electron (minority hole) diffusion coefficient:

$$D_e(N_a,T,r_a,x)=\frac{k_BT}{e}\times\left[200+\frac{8300}{1+\left(\frac{N_a}{1.3\times10^{17}cm^{-3}}\right)^{0.91}}\right]\times\left(\frac{\varepsilon(r_a,x)}{\varepsilon_0(x)}\right)^2\ (cm^2s^{-1}),\qquad(19a)$$

$$D_h(N_d,T,r_d,x)=\frac{k_BT}{e}\times\left[130+\frac{270}{1+\left(\frac{N_d}{8\times10^{17}\ cm^{-3}}\right)^{1.25}}\right]\times\left(\frac{\varepsilon(r_d,x)}{\varepsilon_0(x)}\right)^2\ (cm^2s^{-1}),\qquad(19b)$$

and $\tau_{eB(hB)}(N_{a(d)})$ is the minority electron (minority hole) lifetime in the BR:

$$\tau_{eB}(N_a)^{-1}=\frac{1}{10^{-7}}+3\times10^{-13}\times N_a+1.83\times10^{-31}\times N_a^2,\qquad(20a)$$

$$\tau_{hB}(N_d)^{-1}=\frac{1}{10^{-7}}+11.76\times10^{-13}\times N_d+2.78\times10^{-31}\times N_d^2.\qquad(20b)$$

$J_{Eno(Epo)}$ in the HD[d(a)- X(x)- alloy]ER

In the non-uniformly and heavily doped emitter region of d(a)- X(x) devices, the effective Gaussian d(a)-density profile or the d(a) (majority-e(h)) density, is defined in such the HD[d(a)- X(x) alloy] ER-width W, as[2]:

$$\rho_{d(a)}(y,N^*,W)=N_{d(a)}\times\exp\left\{-\left(\frac{y}{W}\right)^2\times\ln\left[\frac{N^*}{N_{do(ao)}(W)}\right]\right\}\equiv N^*\times\left[\frac{N^*}{N_{do(ao)}(W)}\right]^{-\left(\frac{y}{W}\right)^2},\ 0\le y\le W,$$

$$N_{do(ao)}(W)\equiv7.9\times10^{17}\ (2\times10^5)\times\exp\left\{-\left(\frac{W}{184.2\ (1)\times10^{-7}\ cm}\right)^{1.066\ (0.5)}\right\}\ (cm^{-3}),\qquad(21)$$

where $\rho_{d(a)}(y=0)=N^*$ is the surface d(a)-density, and at the emitter-base junction, $\rho_{d(a)}(y=W)=N_{do(ao)}(W)$, which decreases with increasing W. Further, the "effective doping density" is defined by:

$$N_{d(a)}^*(y,N^*,T,r_{d(a)},x)\equiv\rho_{d(a)}(y)/\exp\left[\frac{\Delta E_{agn(agp)}(\rho_{d(a)},T,r_{d(a)},x)}{k_BT}\right],$$

$$N_{d(a)}^*\left(y=0,N^*,T,r_{d(a)},x\right)\equiv\frac{N^*}{\exp\left[\frac{\Delta E_{agn(agp)}(N^*,T,r_{d(a)},x)}{k_BT}\right]},\ \text{and}$$

$$N_{d(a)}^*\left(y=W,T,r_{d(a)},x\right)\equiv\frac{N_{do(ao)}(W)}{\exp\left[\frac{\Delta E_{agn(agp)}(N_{do(ao)}(W),T,r_{d(a)},x)}{k_BT}\right]},\qquad(22)$$

where the apparent band gap narrowing $\Delta E_{agn(agp)}$ is determined in Equations (16n, 16p), replacing N^* by $\rho_{d(a)}(y, N^*, W)$.

Now, we can define the minority hole (minority electron) transport parameter $F_{h(e)}$, as:

$$F_{h(e)}(y, N^*, T, r_{d(a)}, x) \equiv \frac{N^*}{D_{h(e)} \times \exp\left[\frac{\Delta E_{agn(agp)}}{k_B T}\right]} \; (cm^{-5} \times s), \tag{23}$$

being related to the minority hole (electron) diffusion length, $L_{h(e)}(y, N^*, T, r_{d(a)}, x)$, as:

$$L_{h(e)}^{-2}(y, N^*, T, r_{d(a)}, x) = [\tau_{hE(eE)} \times D_{h(e)}]^{-1} = (C \times F_{h(e)})^2 = \left(C \times \frac{N^*_{d(a)}}{D_{h(e)}}\right)^2 = \left(C \times \frac{n^2_{in(ip)}(T, r_{d(a)})}{p_o(n_o) \times D_{h(e)}}\right)^2,$$

where the constant C was chosen to be equal to: 2.0893×10^{-30} (cm^4/s), and finally the minority hole (minority electron) lifetime $\tau_{hE(eE)}$, by:

$$\tau_{hE(eE)} \equiv \frac{1}{D_{h(e)} \times L^{-2}_{h(e)}} = \frac{1}{D_{h(e)} \times (C \times F_{e(h)})^2}. \tag{24}$$

Then, under low-level injection, in the absence of external generation, and for the steady-state case, we can define the minority-h(e) density by:

$$p_o(y)[n_o(y)] \equiv \frac{n^2_{in(ip)}}{N^*_{d(a)}(y = W, T, r_{d(a)}, x)}, \tag{25}$$

and a normalized excess minority-h(e) density u(x) or a relative deviation between $p(y)[n(y)]$ and $p_o(y)[n_o(y)]$.

$$u(y) \equiv \frac{p(y)[n(y)] - p_o(y)[n_o(y)]}{p_o(y)[n_o(y)]}, \tag{26}$$

which must verify the two following boundary conditions as:

$$u(y = 0) \equiv \frac{-J_h(y = 0)[J_e(y = 0)]}{eS \times p_o(y = 0)[n_o(y = 0)]},$$

$$u(y = W) = \exp\left(\frac{V}{n_{I(II)}(V) \times V_T}\right) - 1.$$

Here, $n_{I(II)}(V)$ is the photovoltaic conversion factor, being determined later, $S\,(\frac{cm}{s})$ is the surface recombination velocity at the emitter contact, V is the applied voltage, $V_T \equiv (k_B T/e)$ is the thermal voltage, and the minority-hole (electron) current density $J_{h(e)}(y, r_{d(a)}, x)$.

Further, from the Fick's law for minority hole (electron)-diffusion equations, one has[1,2]:

$$J_{h(e)}(y, N^*, T, r_{d(a)}, x) = \frac{-e(+e) \times n^2_{in(ip)}}{F_{h(e)}(y)} \times \frac{du(y)}{dy} = \frac{-e(+e) n^2_{in(ip)} D_{h(e)}(N^*, r_{d(a)}, x)}{N^*_{d(a)}(y, N^*, T, r_{d(a)}, x)} \times \frac{du(y)}{dy}, \tag{27}$$

where $N^*_{d(a)}(y, r_{d(a)}, x)$ is given in Eq. (22), $D_{h(e)}$ and $F_{h(e)}$ are determined respectively in Equations (19) and (23), and from the minority-hole (electron) continuity equation as: $N^*_{d(a)}(y, N^*, T, r_{d(a)}, x)$

$$\frac{dJ_{h(e)}(y,N^*,T,r_{d(a)},x)}{dy} = -e(+e) \times n^2_{i\,n(p)} \times \frac{u(y)}{F_{h(e)}(y)\times L^2_{h(e)}(y)} = -e(+e) \times n^2_{i\,n(p)} \times \frac{u(y)}{N^*_{d(a)}(y,N^*,T,r_{d(a)},x)\times \tau_{hE(eE)}}, \quad (28)$$

Therefore, the following second-order differential equation is obtained:

$$\frac{d^2u(y)}{dy^2} - \frac{dF_{h(e)}(y)}{dy} \times \frac{du(y)}{dy} - \frac{u(y)}{L^2_{h(e)}(y)} = 0, \quad (29)$$

Then, taking into account the two above boundary conditions given in Eq. (26), one thus gets the general solution of this Eq. (29), as:

$$u(y) = \frac{\sinh(P(y)) + I(W,S)\times\cosh(P(y))}{\sinh(P(W)) + I(W,S)\times\cosh(P(W))} \times \left(\exp\left(\frac{V}{n_{I(II)}(V)\times V_T}\right) - 1\right), \quad (30)$$

where the factor $I(W,S)$ is determined by: $D_{h(e)}(N_d, T, r_{d(a)}, x)$

$$I(T, r_{d(a)}, x, W, S) = \frac{D_{h(e)}(y=W, N_{do(ao)}(W), T, r_{d(a)}, x)}{S\times L_{h(e)}(y=W, N_{do(ao)}(W), T, r_{d(a)}, x)}. \quad (31)$$

Further, since $\frac{dP(y)}{dy} \equiv C \times F_{h(e)}(y) = \frac{1}{L_{h(e)}(x)}$, $C = 2.0893 \times 10^{-30}\ (cm^4/s)$, for the X(x)-alloy, being an empirical parameter, chosen for each crystalline semiconductor, P(y) is thus found to be defined by: $P(y) \equiv \int_0^y \frac{dy}{L_{h(e)}(y)}$, $0 \le y \le W$, $P(y=W) \equiv \left(\frac{1}{W} \times \int_0^W \frac{dy}{L_{h(e)}(y)}\right) \times W \equiv \frac{W}{L^*_{h(e)}(y)} = \frac{L_{h(e)}(y)}{L^*_{h(e)}(y)} \times \frac{W}{L_{h(e)}(y)}$, (32)

where $L^*_{h(e)}(y)$ is the effective minority hole (minority electron) diffusion length. Further, the minority-hole (electron) current density injected into the HD[d(a)- X(x) alloy] ER is found to be given by: $J_{h(e)}(y, W, N^*, T, r_{d(a)}, x, S, V) = -J_{Eno}(y, W, N^*, T, r_d, x, S)\ [J_{Epo}(y, W, N^*, T, r_a, x, S)] \times \left(\exp\left(\frac{V}{n_{I(II)}(V)\times V_T}\right) - 1\right)$, (33)

where $J_{Eno(Epo)}$ is the saturation minority hole (minority electron) current density,

$$J_{Eno(Epo)}(y, W, N^*, T, r_{d(a)}, x, S) = \frac{en^2_{in(ip)}\times D_{h(e)}}{N^*_{d(a)}(y,N^*,T,r_{d(a)},x)\times L_{h(e)}} \times \frac{\cosh(P(x)) + I(W,S)\times\sinh(P(x))}{\sinh(P(W)) + I(W,S)\times\cosh(P(W))}. \quad (34)$$

In the following, we will denote P(W) and $I(W,S)$ by P and I, for a simplicity. So, Eq. (30) gives:

$$J_{Eno(Epo)}(y=0, W, N^*, T, r_{d(a)}, x, S) = \frac{en^2_{in(ip)}\times D_{h(e)}}{N^*_{d(a)}(y,N^*,T,r_{d(a)},x)\times L_{h(e)}} \times \frac{1}{\sinh(P) + I\times\cosh(P)}, \quad (35)$$

$$J_{Eno(Epo)}(y=W, W, N^*, T, r_{d(a)}, x, S) = \frac{en^2_{i\,n(ip)}\times D_{h(e)}}{N^*_{d(a)}(y=W,N^*,T,r_{d(a)},x)\times L_{h(e)}} \times \frac{\cosh(P) + I\times\sinh(P)}{\sinh(P) + I\times\cosh(P)}, \quad (36)$$

and then,

$$\frac{J_{h(e)}(y=0,W,N^*,T,r_{d(a)},x,S,V)}{J_{h(e)}(y=W,W,N^*,T,r_{d(a)},x,S,V)} = \frac{J_{Eno(Epo)}(y=0,W,N^*,T,r_{d(a)},x,S)}{J_{Eno(Epo)}(y=W,W,N^*,T,r_{d(a)},x,S)} = \frac{1}{\cosh(P) + I\times\sinh(P)}. \quad (37)$$

Now, if defining the effective excess minority-hole (electron) charge storage in the emitter region by:

$Q^*_{h(e)}(y = W, N^*, T, r_{d(a)}, x) \equiv \int_0^W +e(-e) \times u(y) \times p_o(y)[n_o(y)] \times \frac{\tau_{hE(eE)}(N^*,T,r_{d(a)},x)}{\tau_{hE(eE)}(\rho_{d(a)}(x),T,r_{d(a)},x)} dy$, and the effective minority hole (minority electron) transit time [htt(ett)] by:

$\tau^{*}_{htt(ett)}(y=W,W,N^{*},r_{d(a)},x,S) \equiv Q^{*}_{h(e)}(y=W,N^{*},T,r_{d(a)},x)/J_{Eno(Epo)}(y=W,W,N^{*},T,r_{d(a)},x,S)$, and from Equations (24, 31), one obtains:

$$\frac{\tau^{*}_{htt(ett)}(y=W,W,N^{*},T,r_{d(a)},x,S)}{\tau_{hE(eE)}} \equiv 1-\frac{J_{Eno(Epo)}(y=0,W,N^{*},T,r_{d(a)},x,S)}{J_{Eno(Epo)}(y=W,W,N^{*},T,r_{d(a)},x,S)} = 1-\frac{1}{\cosh(P)+I\times\sinh(P)}. \quad (38)$$

Now, some important results can be obtained and discussed below.

As $P \ll 1$ (or $W \ll L_{h(e)}$) and $S \to \infty$, $I \equiv I(W,S) = \frac{D_{h(e)}(N_{do(ao)}(W),T,r_{d(a)},x)}{S\times L_{h(e)}(N_{do(ao)}(W),T,r_{d(a)},x)} \to 0$, from Eq. (38), one has: $\frac{\tau^{*}_{htt(ett)}(y=W,W,N^{*},T,r_{d(a)},x,S)}{\tau_{hE(eE)}} \to 0$, suggesting a completely transparent emitter region (CTER)-case, where, from Eq. (36), one obtains:

$$J_{Eno(Epo)}(y=W,N^{*},T,r_{d(a)},x,S\to\infty) \to \frac{e n^{2}_{in(ip)}\times D_{h(e)}}{N^{*}_{d(a)}(y=W,N^{*},T,r_{d(a)},x)\times L_{h(e)}} \times \frac{1}{P(W)}. \quad (39)$$

Further, as $P \gg 1$ (or $W \gg L_{h(e)}$) and $S \to 0$, $I \equiv I(y=W,r_{d(a)},x,S) = \frac{D_{h(e)}(N_{do(ao)}(W),T,r_{d(a)},x)}{S\times L_{h(e)}(N_{do(ao)}(W),T,r_{d(a)},x)} \to \infty$, and from Eq. (38) one has: $\frac{\tau^{*}_{htt(ett)}(y=W,W,N^{*},T,r_{d(a)},x,S)}{\tau_{hE(eE)}} \to 1$, suggesting a completely opaque emitter region (COER)-case, where, from Eq. (36), one gets:

$$J_{Eno(Epo)}(y=W,N^{*},T,r_{d(a)},x,S\to 0) \to \frac{e n^{2}_{in(ip)}\times D_{h(e)}}{N^{*}_{d(a)}(y=W,N^{*},T,r_{d(a)},x)\times L_{h(e)}} \times \tanh(P). \quad (40)$$

In summary, in the two $n^{+}(p^{+})-p(n)$ X(x)-alloy junction solar cells, the dark carrier-minority saturation current density $J_{oI(oII)}$, defined in Eq. (17), is now rewritten as:

$$J_{oI(oII)}(W,N^{*},T,r_{d(a)},x,S;\ N_{a(d)},r_{a(d)},x) \equiv J_{Eno(Epo)}(W,N^{*},T,r_{d(a)},x,S) + J_{Bpo(Bno)}(N_{a(d)},T,r_{a(d)},x), \quad (41)$$

where $J_{Eno(Epo)}$ and $J_{Bpo(Bno)}$ are determined respectively in Equations (36, 18).

PHOTOVOLTAIC CONVERSION EFFECT AT 300K

Here, in the $n^{+}(p^{+})-p(n)$ X(x) -alloy junction solar cells at T=300 K, denoted respectively by I(II), and for physical conditions, respectively, as:

$$W = 15\ \mu m, N = 10^{20} cm^{-3} (10^{20} cm^{-3}), r_{d(a)}, x, S = 100\ \left(\frac{cm}{s}\right);\ N_{a(d)} = 10^{17}\ cm^{-3},\ r_{a(d)},\ x, \quad (42)$$

we propose, at given open circuit voltages: $V_{ocI1(ocI2)}$ and $V_{ocII1(ocII2)}$, the corresponding data of the short circuit current density $J_{scI(II)}$, in order to formulate our following treatment method of two fix points, as:

at $V_{ocI1(ocI2)}(V) = 0.980\ (1.1272)$, $J_{scI1(scI2)}(mA/cm^{2}) = 27.06\ (29.76)$,

at $V_{ocII1(ocII2)}(V) = 0.980\ (1.03)$, $J_{scII1(scII2)}(mA/cm^{2}) = 24.2\ (29.84)$. (43)

Now, we define the net current density J at T=300 K, obtained for the infinite shunt resistance, and expressed as a function of the applied voltage V, flowing through the $n^+(p^+) - p(n)$ X(x)-alloy junction of solar cells, as:

$$J(V) \equiv J_{ph.}(V) - J_{oI(oII)} \times \left(e^{X_{I(II)}(V)} - 1\right),\ X_{I(II)}(V) \equiv \frac{V}{n_{I(II)}(V)\times V_T},\ X_{I(II)}(V) \equiv \frac{V}{n_{I(II)}(V)\times V_T}, \quad (44)$$

where the function $n_{I(II)}(V)$ is the photovoltaic conversion factor (PVCF), noting that as $V = V_{oc}$, being the open circuit voltage, $J(V = V_{oc}) = 0$, the photocurrent density is defined by: $J_{ph.}(V = V_{oc}) \equiv J_{scI(scII)}(W, N^*, T, r_{d(a)}, x, S;\ N_{a(d)}, T, r_{a(d)}, x, V_{oc})$, for $V_{oc} \geq V_{ocI1(ocII1)}$.

Therefore, the photovoltaic conversion effect occurs, according to:

$$J_{scI(scII)}(W, N^*, T, r_{d(a)} x, S;\ N_{a(d)}, T, r_{a(d)}, x, V_{oc}) \equiv J_{oI(oII)}(W, N^*, T, r_{d(a)}, x, S;\ N_{a(d)}, T, r_{a(d)}, x) \times \left(e^{X_{I(II)}(V_{oc})} - 1\right), \quad (45)$$

where $n_{I(II)}(V_{oc}) \equiv n_{I(II)}(W, N^*, T, r_{d(a)}, x, S;\ N_{a(d)}, r_{a(d)}, x, V_{oc})$, and $X_{I(II)}(V_{oc}) \equiv \frac{V_{oc}}{n_{I(II)}(V_{oc})\times V_T}$.

Here, one remarks that (i) for a given V_{oc}, both $n_{I(II)}$ and $J_{oI(II)}$ have the same variations, obtained in the same physical conditions, as observed in the following calculation, (ii) the function $\left(e^{X_{I(II)}(V_{oc})} - 1\right)$ or the PVCF, $n_{I(II)}$, representing the photovoltaic conversion effect, converts the light, represented by $J_{scI(scII)}$, into the electricity, by $J_{oI(oII)}$, and finally, for given $(W, N^*, T, r_{d(a)}, x, S;\ N_{a(d)}, T, r_{a(d)}, x, V_{oc})$-values, $n_{I(II)}(V_{oc})$ is determined.

Now, for $V_{oc} \geq V_{ocI1(ocII1)}$, one can propose the general expressions for the PVCF, in order to get exactly the values of $n_{I1(II1)}(V_{ocI1(ocII1)})$ and $n_{I2(II2)}(V_{ocI2(ocII2)})$, as functions of V_{oc}, by:

$$n_{I(II)}(W, N^*, T, r_{d(a)}, x, S;\ N_{a(d)}, T, r_{a(d)}, x, V_{oc}) = n_{I1(II1)}(V_{ocI1(ocII1)}) + n_{I2(II2)}(V_{ocI2(ocII2)}) \times \left(\frac{V_{oc}}{V_{ocI1(ocII1)}} - 1\right)^{\alpha(\beta)}, \quad (46)$$

where, for example, the values of $\alpha(\beta)$, obtained for $x = (0, 0.5 \text{ and } 1)$, will be reported in Tables 3n and 5p, for these $[X(x) \equiv GaAs_{1-x}P_x]$-alloy junctions.

So, one can determine the general expressions for the fill factors, as:

$$F_{I(II)}(W, N^*, T, r_{d(a)}, x, S; N_{a(d)}, T, r_{a(d)}, x, V_{oc}) = \frac{X_{I(II)}(V_{oc}) - \ln[X_{I(II)}(V_{oc}) + 0.72]}{X_{I(II)}(V_{oc}) + 1}. \quad (47)$$

Finally, the efficiency $\eta_{I(II)}$ can be defined in the $n^+(p^+) - p(n)$ X(x) alloy-junction solar cells, by:

$$\eta_{I(II)}(W, N^*, T, r_{d(a)}, x, S;\ N_{a(d)}, T, r_{a(d)}, x, V_{oc}) \equiv \frac{J_{scI(scII)} \times V_{oc} \times F_{I(II)}}{P_{in.}}, \quad (48)$$

being assumed to be obtained at 1 sun illumination or at AM1.5G spectrum $(P_{in.} = 0.100\ \frac{W}{cm^2})$.

It should be noted that the maximal values of $\eta_{I(II)}$, $\eta_{Imax.(IImax.)}$, are obtained at the corresponding ones of $V_{oc} = V_{ocI(ocII)}$, at which $\left(\frac{\partial \eta_{I(II)}(W, N^*, T, r_{d(a)}, x, S; N_{a(d)}, r_{a(d)}, x, V_{oc})}{\partial V_{oc}}\right)_{V_{oc}=V_{ocI(ocII)}} = 0$, as those given in next Tables 3n and 5p in Appendix 1, being marked in bold. Further, from the well-known Carnot's theorem, being obtained by the second principle in thermodynamics, or by the entropy law, the maximum efficiency of a heat engine operating between hot (**H**) and cold (**C**) reservoirs is the ratio of the temperature difference between the reservoirs, $T_H - T_C$, $T_C \equiv T = 300\,K$, to the H-reservoir temperature, T_H, expressed as:

$$\eta_{I(II)}(T, V_{oc}) \leq \eta_{Imax.(IImax.)}(T, V_{oc} = V_{ocI(ocII)}) \equiv \eta_{Carnot} = \frac{T_H - T_C}{T_H}, \quad (49)$$

for a simplicity, noting that both $\eta_{Imax.(IImax.)}$ and T_H depend on $(W, N^*, T, r_{d(a)}, x, S;\ N_{a(d)}, r_{a(d)}, x, V_{ocI(ocII)})$-parameters.

NUMERICAL RESULTS AND CONCLUDING REMARKS

We will respectively consider the two following cases of $n^+(p^+) - p(n)$ -junctions such as: HD (As; Sn) X(x) alloy ER – LD (Mg ; Cd) X(x) – alloy BR –case, according to: 2 (n^+p) – junctions denoted by: (As^+Mg, Sn^+Cd), and

HD (Mg ; Cd) X(x) alloy ER – LD (As; Sn) X(x) – alloy BR –case, according to: 2 (p^+n) – junctions denoted by: (Mg^+As, Cd^+Sn).

Now, by using the physical conditions, given in Eq. (42), we can determine various photovoltaic conversion coefficients as follows.

Firs case: HD [As; Sn] X(x) – Alloy ER – LD [Mg ; Cd] X(x) – Alloy BR

Here, there are the 2 $(n^+p) - X(x)$ junctions, being denoted by: (As^+Mg, Sn^+Cd).

Then, the numerical results of $\frac{\tau^*_{htt}}{\tau_{hE}}$, J_{Bpo}, J_{Eno} and J_{oI}, are calculated using Equations (38), (18), (36) and (41), respectively, and obtained, as those given in Table 2n in Appendix 1. Further, those of n_I, J_{scI}, F_I, η_I, and T_H, are computed, using Equations (46, 45, 47, 48, 49), respectively, and reported in the following Table 3n in Appendix 1.

Tables 2n and 3n in Appendix 1

Second case: HD [Mg; Cd] X(x) – Alloy ER – LD [As, Sn] X(x) – Alloy BR

Here, there are 2 $(p^+n) - X(x)$-junctions, being denoted by: (Mg^+As, Cd^+Sn).

Then, the numerical results of $\frac{\tau_{ett}^{*}}{\tau_{eE}}$, J_{Bno}, J_{Epo} and J_{oII}, are calculated using Equations (38), (18), (36) and (41), respectively, and obtained, as those given in Table 4p in Appendix 1. Further, those of n_{II}, J_{scII}, F_{II}, η_{II}, and T_H, are computed, using Equations (46, 45, 47, 48, 49), respectively, and reported in the following Table 5p in Appendix 1.

Tables 4p and 5p in Appendix 1

Finally, some concluding remarks are obtained and discussed as follows.

(1) In Table 3n, for the $n^+ - p$ $GaP_{1-x}As_x$ –alloy junction solar cell and for $r_{Sn(Cd)}$-radius, one obtains with increasing x=(0, 0.5, 1): $\eta_{Imax.}(\searrow)$= **32.83 %**, 31.96 %, 31.15 %, according to $T_H(\searrow) = \mathbf{446.6\ K}, 440.9\ K, 435.7\ K$, at $V_{ocI} = \mathbf{1.06\ V}, 1.06\ V, 1.07\ V$, respectively.

(2) In Table 5p, for the $p^+ - n$ $GaP_{1-x}As_x$ –alloy junction solar cell and for $r_{Cd(Sn)}$-radius, one obtains with increasing x=(0, 0.5, 1): $\eta_{IImax.}(\nearrow)$= 32.51 %, 32.51 %, **33.07 %**, according to $T_H(\nearrow) = 444.5\ K, 444.5\ K, \mathbf{448.2\ K}$, at $V_{ocII}(V)[> V_{ocI}(V)] = 1.17\ V, 1.18\ V, 1.20\ V$, respectively, suggesting that such $\eta_{Imax.(IImax.)}$-and-T_H variations depend on $V_{ocII}(V)[> V_{ocI}(V)] -$ ones.

(3) Finally, as noted in above remarks (1) and (2), for x=1, the $GaP_{1-x}As_x$ –alloy becomes the GaAs-one, and therefore, $\eta_{Imax.}$=31.15 % and $\eta_{IImax.}$=33.07 %, which can be compared with the corresponding results obtained by Moon et al.[6] and Green et al.[4] for the single-junction GaAs thin-film solar cell, 22.08 % and 29.71 %, respectively, suggesting that in order to obtain the highest efficiencies, the $GaP_{1-x}As_x$-alloy junction solar cells could be chosen rather than the crystalline GaAs-junction solar cell.

REFERENCES

1. H. Van Cong, "New Critical Impurity Densities in Metal-Insulator Transition, Obtained in n(p)-Type Degenerate [$GaP_{1-x}As_x(Te_x, Sb_x)$]-Crystalline Alloys, being just That of Carriers Localized in Exponential Band Tails. (IV)", World Journal of Engineering Research and Technology, 2024; 10(5): XX-XX.
2. H. Van-Cong, "Maximal Efficiencies in New Single GaAs(1−x) P(x) - Alloy Junction Solar Cells at 300 K". European Journal of Theoretical and Applied Sciences, 2024; 2(1): 394-414.

3. H. Van Cong, “Effects of donor size and heavy doping on optical, electrical and thermoelectric properties of various degenerate donor-silicon systems at low temperatures,” American Journal of Modern Physics, 2018; 7: 136-165; “Accurate expressions for optical coefficients, due to the impurity-size effect, and obtained in n(p)-type degenerate Si crystals, taking into account their correct asymptotic behavior, as the photon energy E (→ ∞),” SCIREA J. Phys., 2023; 8: 172-197.
4. M.A. Green et al., “Solar cell efficiency tables (version 60)”, Prog. Photovolt. Res. & Appl., 2022; 30: 687-701.
5. C. Kittel, “Introduction to Solid State Physics”, Wiley, New York, 1976; 84-100.
6. S. Moon et al., “Highly efficient single GaAs thin-film solar cell on flexible substrate”, Sci. Rep., 2016; 6: 30107.
7. H. Van Cong et al., “Optical bandgap in various impurity-Si systems from the metal-insulator transition study”, Physica B, 2014; 436: 130-139.
8. H. Van Cong & G. Debiais, “A simple accurate expression of the reduced Fermi energy for any reduced carrier density”, J. Appl. Phys., 1993; 73: 1545-1546.
9. H. Van Cong et al., “Size effect on different impurity levels in semiconductors”, Solid State Communications, 1984; 49: 697-699.
10. H. Van Cong et al., “Optical bandgap in various impurity-Si systems from the metal-insulator transition study,” Physica B, 2014; 436: 130-139; H. Stupp et al., Phys. Rev. Lett., 1993; 71: 2634; P. Dai et al., Phys. Rev. B, 1992; 45: 3984.
11. H. Van Cong, “Accurate expressions for optical coefficients, given in n(p)-type degenerate Ge-crystals, due to the impurity-size effect, and obtained from an improved Forouhi-Bloomer parameterization model,” SCIREA J. Phys., 2023; 8: 255-279.

APPENDIX 1

Table 1: In the **$GaP_{1-x}As_x$**-alloy the numerical results of $B_{do(ao)}$, ε, $E_{gno(gpo)}$, $N_{CDn(CDp)}$, $E_{gin(gip)}(r_{d(a)}, x, T)$, and $\eta_{n(p)}(u)$, $u(N^*, T, x) \equiv \frac{N^*}{N_{c(v)}(T,x)}$, are computed for physical conditions, given in Eq. (42), using Equations (5), (8a, 8b), (9a), (10), and (12), respectively. Here, on notes that: (i) $N = 10^{20} cm^{-3}$ and T=300 K, (ii) $N^* \equiv N^*(N, r_{d(a)}, x) \equiv N - N_{CDn(NDp)}(r_{d(a)}, x)$, given in Eq. (9d), and finally (iii) in the limiting conditions: these numerical results are reduced to those given in GaP-crystal for x=0, and to those given in the GaAs-alloy for x=1.

Donor	**P**	As
r_d (nm) ↗	**r_{do}=0.110**	0.118
x ↗	0, 0.5, 1	0, 0.5, 1
$B_{do}(x)$ in 10^9 (N/m^2) ↘	4.123179, 2.60924, 1.4960608	
$\varepsilon(r_d, x)$ ↘	**11.1**, 12.115, **13.13**	10.83572, 11.82655, 12.817384
$E_{gno}(r_d, x)$ eV ↗	**1.796**, 1.658, **1.52**	1.796708, 1.658448, 1.5202571
$N_{CDn}(r_d, x)$ in 10^{16} cm^{-3} ↗	16.859958, 5.5552466, 1.3330088	18.123934, 5.9717184, 1.4329432
$E_{gin}(r_d, x, T)$ in eV	1.72599, 1.57473, 1.42348	1.7267, 1.57518, 1.42374
$\eta_n \gg 1$ **(degenerate case)** ↘	23.395, 31.027, 46.051	23.393, 31.026, 46.051
Donor	Sb	Sn
r_d (nm) ↗	0.136	0.140
x ↗	0, 0.5, 1	0, 0.5, 1
$\varepsilon(r_d, x)$ ↘	8.868820, 9.679798, 10.490775	8.3478503, 9.111190, 9.8745293
$E_{gno}(r_d, x)$ eV ↗	1.8041281, 1.663144, 1.5229492	1.8070212, 1.664974, 1.5239990
$N_{CDn}(r_d, x)$ in 10^{16} cm^{-3} ↗	33.054297, 10.891176, 2.6133913	39.637063, 13.060155, 3.1338483
$E_{gin}(r_d, x, T)$ in eV	1.73412, 1.57988, 1.42643	1.73701, 1.58171, 1.42748
$\eta_n \gg 1$ **(degenerate case)** ↘	23.370, 31.016, 46.047	23.360, 31.012, 46.046
Acceptor	**Ga**	Mg
r_a (nm) ↗	**r_{ao}=0.126**	0.140
x ↗	0, 0.5, 1	0, 0.5, 1
$B_{ao}(x)$ in 10^9 (N/m^2) ↘	1.055177, 0.700649, 0.4388991	

$\varepsilon(r_a, x)$ ↘	**11.1**, 12.115, **13.13**	10.5002, 11.4604, 12.42055
$E_{gpo}(r_a, x)$ eV ↗	**1.796**, 1.658, **1.52**	1.8024849, 1.66231, 1.5226974
$N_{CDp}(r_a, x)$ in 10^{18} cm^{-3} ↗	9.5926026, 3.6514435, 1.142563	11.332043, 4.3135651, 1.3497457
$E_{gip}(r_a, x, T)$ in eV ↗	1.726, 1.5747, 1.4235	1.7325, 1.579, 1.4262
$\eta_p \gg 1$ **(degenerate case)** ↘	5.9036, 7.6634, 10.4814	5.8328, 7.6298, 10.4671
Acceptor	In	Cd
r_a (nm) ↗	0.144	0.148
x ↗	0, 0.5, 1	0, 0.5, 1
$\varepsilon(r_a, x)$ ↘	10.143959, 11.0715, 11.999115	9.7367823, 10.62713, 11.51747
$E_{gpo}(r_a, x)$ eV ↗	1.8068933, 1.665233, 1.5245311	1.8125359, 1.66898, 1.5268781
$N_{CDp}(r_a, x)$ in 10^{18} cm^{-3} ↗	12.568487, 4.7842197, 1.4970169	14.212125, 5.4098739, 1.6927886
$E_{gip}(r_a, x,)$ in eV ↗	1.7369, 1.582, 1.428	1.7425, 1.5857, 1.4304
$\eta_p \gg 1$ **(degenerate case)** ↘	5.7822, 7.6059, 10.4570	5.7146, 7.5741, 10.4434

Table 2n: In the HD [(As; Sn)- $GaP_{1-x}As_x$-alloy] ER-LD[(Mg; Cd)-$GaP_{1-x}As_x$-alloy] BR, for physical conditions given in Eq. (42) and for a given x, our numerical results of $\frac{\tau^{\pm}_{htt}}{\tau_{hE}}$, J_{Bpo}, J_{Eno} and J_{oI}, are computed, using Equations (38), (18), (36) and (41), respectively, noting that J_{oI} decreases strongly with increasing $r_{d(a)}$-radius for given x, but it increases strongly with increasing x for given $r_{d(a)}$-radius, being new results.

n^+p	As^+Mg	Sn^+Cd
Here, **x=0** for the (As^+Mg, Sn^+Cd)-junctions, and from Eq. (38), one obtains: $\frac{\tau^{\pm}_{htt}}{\tau_{hE}} = (0, 0)$ suggesting a completely transparent condition.		
J_{Bpo} in 10^{-24} (A/cm^2) ↘	3.7256	3.4547
J_{Eno} in 10^{-29} (A/cm^2) ↘	2.4794	0.1204
J_{oI} in 10^{-24} (A/cm^2) ↘	3.7256	3.4547

Here, **x=0.5** for the (As^+Mg, Sn^+Cd)-junctions, and from Eq. (38), one obtains: $\frac{\tau^*_{htt}}{\tau_{hE}} = (0, 0)$ suggesting a completely transparent condition.

J_{Bpo} in 10^{-22} (A/cm^2) ↘	6.9673	6.4608
J_{Eno} in 10^{-26} (A/cm^2) ↘	1.6784	0.0176
J_{oI} in 10^{-22} (A/cm^2) ↘	6.9675	6.4608

Here, **x=1** for the (As^+Mg, Sn^+Cd)-junctions, and from Eq. (38), one obtains: $\frac{\tau^*_{htt}}{\tau_{hE}} = (0, 0)$ suggesting a completely transparent condition.

J_{Bpo} in 10^{-20} (A/cm^2) ↘	9.4699	8.7814
J_{Eno} in 10^{-22} (A/cm^2) ↘	8.9188	0.0017
J_{oI} in 10^{-20} (A/cm^2) ↘	9.5592	8.7814

Table 3n: In the HD [(As; Sn)- $GaP_{1-x}As_x$-alloy] ER-LD[(Mg; Cd)-$GaP_{1-x}As_x$-alloy] BR, for physical conditions given in Eq. (42) and for a given x, our numerical results of n_I, J_{scI}, F_I, η_I, and T_H, are computed, using Equations (46, 45, 47, 48, 49), respectively, noting that both $\eta_{Imax.}$ and T_H, marked in bold, increase with increasing x for given $r_{d(a)}$, being new results.

$V_{oc}(V)$	n_I	$J_{scI}(\frac{mA}{cm^2})$	$F_I(\%)$	$\eta_I(\%)$
Here, **x=0**. For the (As^+Mg, Sn^+Cd) junctions, the value of α given in Eq. (46) is 1.0805.				
n^+p	As^+Mg; Sn^+Cd	As^+Mg; Sn^+Cd	As^+Mg; Sn^+Cd	As^+Mg; Sn^+Cd
0.980	0.753; 0.752	27.06; 27.06	90.39; 90.40	23.97; 23.97
1.05	0.803; 0.802	34.60; 34.47	90.43; 90.44	32.72; 32.73
1.06	0.811; 0.809	34.24; 34.25	90.43; 90.44	**32.82; 32.83**
			$V_{ocI} = 1.06$ V	**446.5; 446.6**=$T_H(K)$
1.07	0.818; 0.817	33.86; 33.87	90.42; 90.43	32.76; 32.78
1.1272	0.864; 0.863	29.76; 29.76	90.40; 90.42	30.33; 30.34
2	1.656; 1.653	0.728; 0.724	89.82; 89.83	1.308; 1.301

Here, **x=0.5**. For the (As^+Mg, Sn^+Cd) junctions, the value of α given in Eq. (46) is $\mathbf{1.08126}$.

n^+p	$As^+Mg; Sn^+Cd$	$As^+Mg; Sn^+Cd$	$As^+Mg; Sn^+Cd$	$As^+Mg; Sn^+Cd$
0.980	0.840; 0.839	27.06; 27.06	89.53; 89.55	23.74; 23.75
1.05	0.896; 0.894	33.82; 33.83	89.57; 89.59	31.80; 31.82
1.06	0.904; 0.809	33.64; 34.25	89.57; 89.59	**31.94**; **31.96**
			$\mathbf{V_{ocI} = 1.06\ V}$	**440.8; 440.9**=$T_H(K)$
1.07	0.913; 0.817	33.32; 33.87	89.57; 89.59	31.93; 31.95
1.1272	0.964; 0.863	29.75; 29.76	89.55; 89.56	30.03; 30.04
2	1.847; 1.653	1.064; 0.724	88.92; 88.93	1.893; 1.883

Here, **x=1**. For the (As^+Mg, Sn^+Cd) junctions, the value of α given in Eq. (46) is $\mathbf{1.0822}$.

n^+p	$As^+Mg; Sn^+Cd$	$As^+Mg; Sn^+Cd$	$As^+Mg; Sn^+Cd$	$As^+Mg; Sn^+Cd$
0.980	**0.943**; **0.941**	27.06; 27.06	88.56; 88.58	23.49; 23.49
1.06	1.015; 1.013	33.10; 33.11	88.60; 88.62	31.09; 31.11
1.07	1.025; 1.023	32.84; 32.85	88.60; 88.62	**31.13**; **31.15**
			$\mathbf{V_{ocI} = 1.07\ V}$	**435.6; 435.7**=$T_H(K)$
1.08	1.034; 1.033	32.47; 32.49	88.60; 88.62	31.07; 31.09
1.1272	1.082; 1.080	29.76; 29.77	88.58; 88.60	29.72; 29.73
2	2.073; 2.069	1.522; 1.512	87.89; 87.91	2.675; 2.659

Table 4p: In the HD [(Mg; Cd)-$\mathbf{GaP_{1-x}As_x}$-alloy] ER-LD[(As; Sn)-$\mathbf{GaP_{1-x}As_x}$-alloy] BR, for physical conditions given in Eq. (42) and for a given x, our numerical results of $\frac{\tau^{*}_{eff}}{\tau_{eR}}$, J_{Bno}, J_{Epo} and J_{oII}, are computed, using Equations (38), (18), (36) and (41), respectively, noting that J_{oII} decreases strongly with increasing $r_{a(d)}$-radius for given x, but it increases strongly with increasing x for given $r_{a(d)}$-radius, being new results.

p^+n	Mg^+As	Cd^+Sn

Here, **x=0,** and for the (Mg^+As, Cd^+Sn)-junctions and from Eq. (34), one obtains: $\frac{\tau^*_{eE}}{\tau_{eE}} = (0, 0)$ suggesting a completely transparent condition.

J_{Bno} in 10^{-24} (A/cm^2) ↘	1.6147	0.8348
J_{Epo} in 10^{-27} (A/cm^2) ↘	1.2926	0.7831
J_{oII} in 10^{-24} (A/cm^2) ↘	1.6160	0.8356

Here, **x=0.5,** and for the (Mg^+As, Cd^+Sn)-junctions and from Eq. (34), one obtains: $\frac{\tau^*_{eE}}{\tau_{eE}} = (0, 0)$ suggesting a completely transparent condition.

J_{Bno} in 10^{-22} (A/cm^2) ↘	2.6082	1.5611
J_{Epo} in 10^{-25} (A/cm^2) ↘	1.2570	0.7875
J_{oII} in 10^{-22} (A/cm^2) ↘	2.6095	1.5619

Here, **x=1,** and for the (Mg^+As, Cd^+Sn) junctions and from Eq. (34), one obtains: $\frac{\tau^*_{eE}}{\tau_{eE}} = (0, 0)$ suggesting a completely transparent condition.

J_{Bno} in 10^{-20} (A/cm^2) ↘	3.1831	2.1219
J_{Epo} in 10^{-24} (A/cm^2) ↘	7.7128	4.7505
J_{oII} in 10^{-20} (A/cm^2) ↘	3.1839	2.1223

Table 5p: In the HD [(Mg; Cd)-**GaP$_{1-x}$As$_x$**-alloy] ER-LD[(As; Sn)-**GaP$_{1-x}$As$_x$**-alloy] BR, for physical conditions given in Eq. (42) and for a given x, our numerical results of n_{II}, J_{scII}, F_{II}, η_{II}, and T_H, are computed, using Equations (46, 45, 47, 48, 49), respectively, noting that both $\eta_{IImax.}$ and T_H, marked in bold, increase with increasing x for given $r_{a(d)}$, being new results.

$V_{oc}(V)$	n_{II}	$J_{scII}(\frac{mA}{cm^2})$	$F_{II}(\%)$	$\eta_{II}(\%)$
Here, **x=0**. For the (Mg^+As, Cd^+Sn)-junctions, the value of β given in Eq. (46) is $\mathbf{1.0452}$.				
p^+n	$Mg^+As; Cd^+Sn$	$Mg^+As; Cd^+Sn$	$Mg^+As; Cd^+Sn$	$Mg^+As; Cd^+Sn$

0.980	0.742; 0.733	24.20; 24.20	90.50; 90.59	21.46; 21.48
1.03	0.777; 0.767	29.90; 29.98	90.53; 90.62	27.88; 27.98
1.16	0.874; 0.863	30.84; 30.92	90.53; 90.63	32.38; 32.51
1.17	0.882; 1.036	30.58; 33.14	90.53; 88.60	**32.39**; **32.51**
			V_{ocII} = 1.17 V	**443.7; 444.5**=T_H(K)
1.18	0.890; 1.083	30.29; 33.14	90.53; 88.60	32.36; 32.47
2	1.553; 3.315	7.035; 33.14	90.31; 88.60	12.71; 12.50

Here, **x=0.5**. For the (Mg^+As, Cd^+Sn)-junctions, the value of β given in Eq. (46) is 1.0476.

p^+n	$Mg^+As; Cd^+Sn$	$Mg^+As; Cd^+Sn$	$Mg^+As; Cd^+Sn$	$Mg^+As; Cd^+Sn$
0.980	0.824; 0.815	24.20; 24.20	89.69; 89.78	21.27; 21.29
1.03	0.863; 0.853	29.74; 29.80	89.72; 89.81	27.48; 27.57
1.17	0.979; 0.968	30.84; 30.92	89.73; 89.82	32.39; 32.49
1.18	0.988; 0.977	30.60; 30.67	89.73; 89.82	**32.40**; **32.51**
			V_{ocII} = 1.18 V	**443.8; 444.5**=T_H(K)
1.19	0.996; 0.985	30.34; 33.40	89.73; 89.82	32.39; 32.49
2	1.724; 1.705	8.022; 7.915	89.49; 89.58	14.36; 14.18

Here, **x=1**. For the (Mg^+As, Cd^+Sn)-junctions, the value of β given in Eq. (46) is 1.0519.

p^+n	$Mg^+As; Cd^+Sn$	$Mg^+As; Cd^+Sn$	$Mg^+As; Cd^+Sn$	$Mg^+As; Cd^+Sn$
0.980	0.921; 0.912	24.20; 24.20	88.77; 88.86	21.05; 21.07
1.03	0.963; 0.953	29.82; 29.88	88.81; 88.90	27.28; 27.36
1.19	1.111; 1.100	31.17; 31.24	88.82; 88.91	32.95; 33.05
1.20	1.121; 1.110	30.93; 30.99	88.82; 88.91	**32.97**; **33.07**
			V_{ocII} = 1.20 V	**447.6; 448.2**=T_H(K)
1.21	1.130; 1.119	30.66; 30.72	88.82; 88.90	32.96; 33.05
2	1.925; 1.906	9.071; 8.974	88.56; 88.65	16.07; 15.91